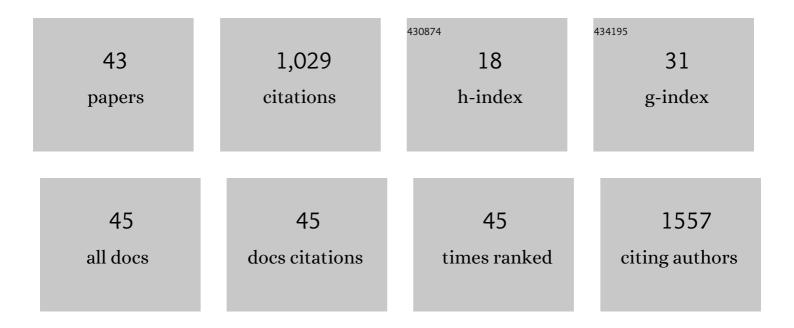
Jongho Jeon

List of Publications by Year in descending order

Source: https://exaly.com/author-pdf/2532512/publications.pdf Version: 2024-02-01



#	Article	IF	CITATIONS
1	Tumor Targeting and Imaging Using Cyclic RGDâ€PEGylated Gold Nanoparticle Probes with Directly Conjugated Iodineâ€125. Small, 2011, 7, 2052-2060.	10.0	173
2	Efficient Method for Site-Specific ¹⁸ F-Labeling of Biomolecules Using the Rapid Condensation Reaction between 2-Cyanobenzothiazole and Cysteine. Bioconjugate Chemistry, 2012, 23, 1902-1908.	3.6	63
3	Review of Therapeutic Applications of Radiolabeled Functional Nanomaterials. International Journal of Molecular Sciences, 2019, 20, 2323.	4.1	61
4	Comparison of Two Site-Specifically ¹⁸ F-Labeled Affibodies for PET Imaging of EGFR Positive Tumors. Molecular Pharmaceutics, 2014, 11, 3947-3956.	4.6	54
5	Efficient bioremediation of radioactive iodine using biogenic gold nanomaterial-containing radiation-resistant bacterium, Deinococcus radiodurans R1. Chemical Communications, 2017, 53, 3937-3940.	4.1	48
6	Preclinical Kinetic Analysis of the Caspase-3/7 PET Tracer ¹⁸ F-C-SNAT: Quantifying the Changes in Blood Flow and Tumor Retention After Chemotherapy. Journal of Nuclear Medicine, 2015, 56, 1415-1421.	5.0	47
7	Recent Advances in Bioorthogonal Click Chemistry for Efficient Synthesis of Radiotracers and Radiopharmaceuticals. Molecules, 2019, 24, 3567.	3.8	44
8	Efficient and selective removal of radioactive iodine anions using engineered nanocomposite membranes. Environmental Science: Nano, 2017, 4, 2157-2163.	4.3	37
9	Silver Nanomaterial-Immobilized Desalination Systems for Efficient Removal of Radioactive Iodine Species in Water. Nanomaterials, 2018, 8, 660.	4.1	34
10	Quantification of inhaled aerosol particles composed of toxic household disinfectant using radioanalytical method. Chemosphere, 2018, 207, 649-654.	8.2	32
11	Efficient method for iodine radioisotope labeling of cyclooctyne-containing molecules using strain-promoted copper-free click reaction. Bioorganic and Medicinal Chemistry, 2015, 23, 3303-3308.	3.0	27
12	Gold-Nanoparticle-Immobilized Desalting Columns for Highly Efficient and Specific Removal of Radioactive Iodine in Aqueous Media. ACS Applied Materials & Interfaces, 2016, 8, 29227-29231.	8.0	24
13	Removal of Hexavalent Chromium(VI) from Wastewater Using Chitosan-Coated Iron Oxide Nanocomposite Membranes. Toxics, 2022, 10, 98.	3.7	24
14	Physiological Effects of Ac4ManNAz and Optimization of Metabolic Labeling for Cell Tracking. Theranostics, 2017, 7, 1164-1176.	10.0	23
15	Critical analysis of radioiodination techniques for micro and macro organic molecules. Journal of Radioanalytical and Nuclear Chemistry, 2016, 309, 859.	1.5	21
16	Highly efficient method for 125I-radiolabeling of biomolecules using inverse-electron-demand Diels–Alder reaction. Bioorganic and Medicinal Chemistry, 2016, 24, 2589-2594.	3.0	19
17	Continuous Flow Removal of Anionic Dyes in Water by Chitosan-Functionalized Iron Oxide Nanoparticles Incorporated in a Dextran Gel Column. Nanomaterials, 2019, 9, 1164.	4.1	19
18	Activatable red emitting fluorescent probe for rapid and sensitive detection of intracellular peroxynitrite. Talanta, 2020, 217, 121053.	5.5	19

Jongho Jeon

#	Article	IF	CITATIONS
19	Removal of Radioactive lodine Using Silver/Iron Oxide Composite Nanoadsorbents. Nanomaterials, 2021, 11, 588.	4.1	19
20	Recent Progress in Technetium-99m-Labeled Nanoparticles for Molecular Imaging and Cancer Therapy. Nanomaterials, 2021, 11, 3022.	4.1	19
21	Synthesis and evaluation of curcumin-based near-infrared fluorescent probes for the in vivo optical imaging of amyloid-β plaques. Bioorganic Chemistry, 2021, 115, 105167.	4.1	17
22	Rapid and Efficient Removal of Anionic Dye in Water Using a Chitosan-Coated Iron Oxide-Immobilized Polyvinylidene Fluoride Membrane. ACS Omega, 2022, 7, 8759-8766.	3.5	17
23	Efficient and stable radiolabeling of polycyclic aromatic hydrocarbon assemblies: in vivo imaging of diesel exhaust particulates in mice. Chemical Communications, 2019, 55, 447-450.	4.1	16
24	A strategy to enhance the binding affinity of fluorophore–aptamer pairs for RNA tagging with neomycin conjugation. Chemical Communications, 2012, 48, 10034.	4.1	15
25	Efficient radiolabeling of rutin with 125I and biodistribution study of radiolabeled rutin. Journal of Radioanalytical and Nuclear Chemistry, 2016, 308, 477-483.	1.5	15
26	Radiosynthesis of 123I-labeled hesperetin for biodistribution study of orally administered hesperetin. Journal of Radioanalytical and Nuclear Chemistry, 2015, 306, 437-443.	1.5	13
27	Effect of Particulate Matter on Human Health, Prevention, and Imaging Using PET or SPECT. Progress in Medical Physics, 2018, 29, 81.	0.3	13
28	Synthesis and evaluation of an 125 I-labeled azide prosthetic group for efficient and bioorthogonal radiolabeling of cyclooctyne-group containing molecules using copper-free click reaction. Bioorganic and Medicinal Chemistry Letters, 2016, 26, 875-878.	2.2	12
29	Discovery of boronic acid-based fluorescent probes targeting amyloid-beta plaques in Alzheimer's disease. Bioorganic and Medicinal Chemistry Letters, 2016, 26, 1784-1788.	2.2	12
30	Development of a Squaraine-Based Molecular Probe for Dual-Modal <i>in Vivo</i> Fluorescence and Photoacoustic Imaging. Bioconjugate Chemistry, 2020, 31, 2607-2617.	3.6	11
31	Radiosynthesis and in vivo evaluation of [125I]2-(4-iodophenethyl)-2-methylmalonic acid as a potential radiotracer for detection of apoptosis. Journal of Radioanalytical and Nuclear Chemistry, 2016, 308, 23-29.	1.5	8
32	Radioprotective effect of hesperetin against ^{ĵ3} -irradiation-induced DNA damage and immune dysfunction in murine splenocytes. Food Science and Biotechnology, 2016, 25, 163-168.	2.6	8
33	Simple and efficient radiolabeling of hyaluronic acid and its in vivo evaluation via oral administration. Journal of Radioanalytical and Nuclear Chemistry, 2015, 305, 139-145.	1.5	7
34	Synthesis, structural characterization and MMA polymerization studies of dimeric 5-coordinate copper(II), cadmium(II), and monomeric 4-coordinate zinc(II) complexes supported by N-methyl-N-((pyridine-2-yl)methyl)benzeneamine. Inorganica Chimica Acta, 2019, 487, 221-227.	2.4	7
35	Radioanalytical Techniques to Quantitatively Assess the Biological Uptake and In Vivo Behavior of Hazardous Substances. Molecules, 2020, 25, 3985.	3.8	7
36	A functionalized nanocomposite adsorbent for the sequential removal of radioactive iodine and cobalt ions in aqueous media. Korean Journal of Chemical Engineering, 2020, 37, 2209-2215.	2.7	7

Jongho Jeon

#	Article	IF	CITATIONS
37	Development of a new thiol-reactive prosthetic group for site-specific labeling of biomolecules with radioactive iodine. Bioorganic and Medicinal Chemistry Letters, 2018, 28, 2875-2878.	2.2	6
38	An Optimized Protocol for the Efficient Radiolabeling of Gold Nanoparticles by Using a ¹²⁵ I-labeled Azide Prosthetic Group. Journal of Visualized Experiments, 2016, , .	0.3	4
39	Technetium-99m-based simple and convenient radiolabeling of Escherichia coli for in vivo tracking of microorganisms. Journal of Radioanalytical and Nuclear Chemistry, 2018, 317, 997-1003.	1.5	4
40	Study on biological distribution of polyhexamethylene guanidine (PHMG), a toxic household chemical, using radiolabeling and molecular imaging tools. Environmental Engineering Research, 2022, 27, 210393-0.	2.5	2
41	Radiosynthesis and preliminary biological evaluation of 99mTc-labeled 2-methyl-2-pentylmalonic acid as an apoptosis imaging agent. Journal of Radioanalytical and Nuclear Chemistry, 2017, 313, 207-215.	1.5	1
42	An Efficient Method for Selective Desalination of Radioactive Iodine Anions by Using Gold Nanoparticles-Embedded Membrane Filter. Journal of Visualized Experiments, 2018, , .	0.3	1
43	Innentitelbild: Positron Emission Tomography Imaging of Drug-Induced Tumor Apoptosis with a Caspase-Triggered Nanoaggregation Probe (Angew. Chem. 40/2013). Angewandte Chemie, 2013, 125, 10584-10584.	2.0	0